Macromolecules

ARTICLE

pubs.acs.org/Macromolecules

Glass Transition Dynamics and Surface Mobility of Entangled Polystyrene Films at Equilibrium

Zhaohui Yang,[†,§] Andrew Clough,[†] Chi-Hang Lam,[‡] and Ophelia K. C. Tsui*[,†]

[†]Department of Physics, Boston University, Boston, Massachusetts 02215, United States

[‡]Department of Applied Physics, Hong Kong Polytechnic University, Hung Hom, Hong Kong

ABSTRACT: There has been continuing effort to understand the cause for the thickness dependence observed in the glass transition dynamics of polymer films. In a previous experiment, we showed that a two-layer model, assuming the films to contain a high-mobility surface layer residing on top of a bulklike inner layer, can explain the thickness dependence found in the viscosity of unentangled polystyrene films. Here, we examine the validity of this model in polystyrene films that are entangled. Unlike the unentangled films, the entangled ones are initially out-of-equilibrium, exhibiting a plateau modulus ∼1/10 times the bulk value. Upon annealing, the viscosity typically grows with time and eventually saturates. For the films with thickness above 20 nm, the saturated viscosity is the same as the bulk and takes ∼5−10 reptation times to reach. We find that the saturated viscosity is fully explainable by the two-layer model. A straightforward interpretation would imply that the surface mobile layer exists at equilibrium and modifies the dynamics of unentangled and entangled polymer films in a similar way.

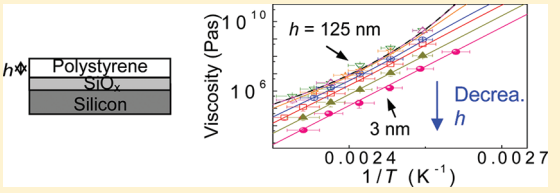

INTRODUCTION

Polymer films have widespread applications, including microelectronics, lubrication, and adhesives, etc. The emergence of nano science and technology has increased the usage of polymer films with thickness in the nanometer range. Studies in the past two decades showed that the properties we know well about polymers in the bulk can be very different when they are confined in nanostructures. One of the most studied phenomena is the noticeable decrease in the glass transition temperature, T_g, with decreasing film thickness, h, of some polymer films with $h <$ ∼100 nm.[1−8] This finding suggests that polymer nanostructures can potentially melt at a temperature substantially below the bulk polymer, so efficient application of polymeric materials in nano science and technology necessitates a good understanding of the dynamics of these materials under nanoconfinement at the glass transition. The most frequently cited model used to explain the thickness dependence (h) of the T_g of polymer nanometer films is the layer model.[1,3,9,10] In this model, the films are portrayed as consisting of a high-mobility surface layer resting on top of a less mobile, largely bulklike inner layer; the overall dynamics of the films and hence the T_g is a result of the interplay between the two. If the surface layer dominates, the T_g is decreased; otherwise, the T_g is enhanced, unchanged, or decreased depending on whether the polymer−substrate interactions are attractive, neutral, or repulsive, respectively. As for how the layer model may produce the $T_g(h)$ found in experiment, it has been a subject of debate for a long time. In a recent experiment,[11] we showed in polystyrene (PS) films cast on silicon that a highly mobile region with thickness no more than 2.3 nm existed at the free surface, and it engendered the T_g reduction by providing an additional, high-mobility flow channel whereby the total mobility of the films can be enhanced. But in that experiment, only unentangled PS films, exhibiting viscous dynamics, were studied, while the dynamics of polymers are known to exhibit viscoelastic behaviors when the molecular weight, M_w, of the polymer is increased above the entanglement molecular weight, M_e.[12,13] In addition, a recent experiment[14] showed that entangled PS films, when not equilibrated, could also exhibit reduced viscosity merely due to the conformation with lesser degree of interchain entanglements inherited by the films when they were fabricated, i.e., during the spin-coating process.[14,15] The out-of-equilibrium conformation was also found to be lasting,[14,16−18] raising concerns about how significant a role a surface mobile layer, if present, may play in the dynamics of entangled PS films. In this study, we measure the evolution in the dynamics of as-cast PS films with $M_w > 10M_e$ upon annealing above the T_g and examine if the surface mobile layer exists when the films reach equilibrium and whether at that point it affects the dynamics of these films as it does in the unentangled films.[11]

EXPERIMENTAL SECTION

The polymer used in this experiment was polystyrene purchased from Scientific Polymer Products (Ontario, NY) with M_w = 212 kg/mol and polydispersity index = 1.08. The substrates were 1.5 × 1.5 cm^2 slides of Si (100) covered with a 102 ± 5 nm thick thermal oxide. Prior to use, the substrates were cleaned in a piranha solution as described before.[16] Thin films of the polymer, with thickness h varied from 2 to 125 nm, were spin-coated onto the substrates from solutions of the polymer in toluene and measured without preannealing. The film thickness was controlled by varying the concentration of the polymer solution and measured by

Received: July 21, 2011
Revised: August 28, 2011
Published: October 04, 2011

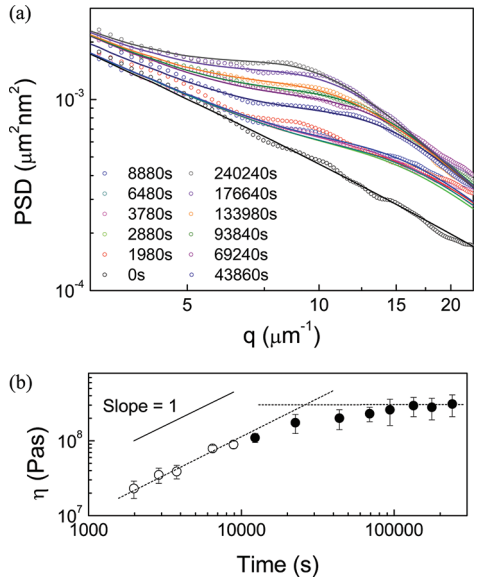

Figure 1. (a) Power spectral density of a 20 nm film upon annealing at 120 °C for various times as shown in the legend. The solid lines are the least-squares fit of the data to eqs 1−3 as described in the text. (b) A plot of the fitted viscosity versus time of the data shown in (a). The open and solid symbols denote the data taken in the rubbery plateau and terminal flow regime, respectively. The solid line is an indicator for slope = 1. The dashed lines are the short- and long-time asymptotes of the data. The time where the asymptotes overlap is taken to be the equilibration time, τ_{eq}.

ellipsometry. The dynamics of the films was determined by monitoring the evolution in the surface topography of the films at different times during the initial stage of dewetting[19−22] when the surface roughness is much less than the film thickness and well before any holes are formed. (In this experiment, the rms roughness is always <0.1h and <0.05h for most of the films studied.) While most of the measurements were taken after quenching the sample to room temperature whereat its surface structure was frozen, no difference in the result was detectable when the measurements were taken in real-time as the film was heated. To measure the surface topography of the films, we used tapping-mode atomic force microscopy (AFM). To facilitate the model analysis (discussed in detail below), we converted the topographic data to its power spectral density (PSD).[19−22] This was done by multiplying the data with a Welch function before Fourier-transforming it.[19−22] The 2-dimensional Fourier spectrum was then radial averaged to give the 1-dimensional PSD.

THEORETICAL ANALYSIS

We have shown that in the initial stage of heating where the height fluctuation is small compared to the film thickness, the PSD ($A_q^2(t)$) of thin polymer films evolves with time t at a temperature T according to the relation[11,16,19,23]

$$A_q^2(t) = A_q^2(0)\exp(2\omega t) + \left[\frac{k_B T}{d^2G(h)/dh^2 + \gamma q^2}\right](1 - \exp(2\omega t)) \quad (1)$$

where k_B is the Boltzmann constant, ω is the relaxation rate of the surface capillary wave with wavevector q, and $G(h)$ and γ are respectively the van der Waals potential[24] and surface tension of the film. By solving the Laplace transform of the Navier−Stokes equation in the lubrication approximation, Safran and Klein derived an expression for $\omega(q)$ for viscoelastic films:[25]

$$\omega = -\frac{h^3}{3\eta(\omega)}\left[\left(\frac{d^2G(h)}{dh^2}\right)q^2 + \gamma q^4\right] \quad (2)$$

For viscoelastic liquids with a short-time shear modulus, μ_0, and single characteristic relaxation time, $\tau_r \equiv 1/\omega_r$,[25] $\eta(\omega) = \mu_0 / (\omega + \omega_r)$. With this, eq 2 can be rewritten as

$$\omega = \frac{\omega_{liq}}{1 - \omega_{liq}\tau_r} \quad (3)$$

where $\omega_{liq} \equiv -(h^3/3\eta)[(dG^2(h)/dh^2)q^2 + \gamma q^4]$ is the relaxation rate of the qth surface capillary mode of purely viscous films with viscosity, $\eta \equiv \mu_0\tau_r$. Equation 3 suggests that $\omega \approx -1/\tau_r$ if $|\omega_{liq}\tau_r| \gg 1$, but crosses over to $\omega \approx \omega_{liq}$ if $|\omega_{liq}\tau_r| \ll 1$. By substituting the sample parameters, we find that $|\omega| < 1/\tau_r$, implying that the capillary modes require a minimum duration of τ_r to relax.[23] So during the initial annealing when $t < \tau_r$, which is also when the film is in the elastic regime, the PSD remains stationary. Upon $t > \tau_r$, the film enters the viscous regime and the PSD evolves with $\omega \approx \omega_{liq}$ as expected given the long-time viscous behavior assumed of the films.

The predicted short-time ($t < \tau_r$) behavior is clearly demonstrated by the PSD's in Figure 1a. The elastic regime can be ascribed to the rubbery plateau regime well-known for entangled polymers.[12] Fredrickson et al.[26] showed that the PSD of a solid film with shear modulus μ_0 and thickness h was given by

$$A_q^2(t) = \text{background} + \frac{k_B T}{d^2G(h)/dh^2 + \gamma q^2 + \frac{3\mu_0}{h^3 q^2}} \quad (4)$$

At the same time, it has been shown[16] that eq 1 can be approximated by

$$A_q^2(t) = \text{background} + \frac{k_B T}{d^2G(h)/dh^2 + \gamma q^2 + \frac{3(\eta(\omega)/2t)}{h^3 q^2}} \quad (5)$$

During the rubbery plateau, the films are elastic and Fredrickson's model (eq 4) should apply. A comparison between eqs 4 and 5 suggests that if we fit the data in the rubbery regime to eq 1 and set $\eta(\omega) = \eta$ (which amounts to setting $\omega = \omega_{liq}$ in eq 3), we should find that the fitted value of η increases linearly with t, and by using $\eta = 2\mu_{plateau}t$, the value of $\mu_{plateau}$ can be deduced.

Beyond the rubbery plateau, the films are viscous. We deduce the viscosity of the films, η, by fitting the PSD's to eqs 1−3 with η treated as the fitting parameter, μ_0 set equal to $\mu_{plateau}$, and the rest of the parameters given the experimental or published values. (In particular, we used the experimental values for h and T, 30 mN/m for γ, and the values published in ref 24 for $dG^2(h)/dh^2$.) We find that a wide range of μ_0 can produce a good fit to the data, as long as μ_0 is large enough that $\mu_0 t/\eta \equiv t/\tau_r > \sim 1$. This shows that the model fitting beyond the rubbery plateau cannot be used to obtain a reliable value of μ_0. But it does for η and the fitted value of η has been found to always fall within a limited range even when μ_0 is varied over its maximum range.

It should be mentioned that this model treats the films as being uniform; that is, $\mu_{plateau}$ and η are both taken to be constants, independent of position. On the other hand, the dynamics of polymer films are well-known to be heterogeneous, especially for

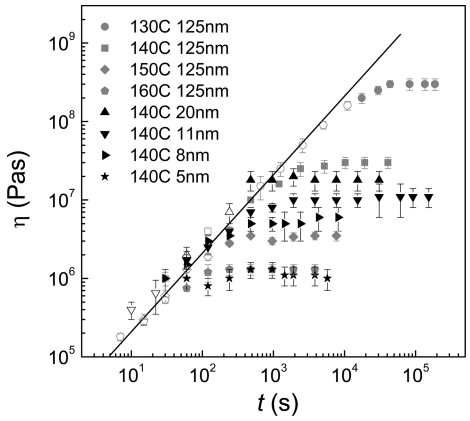

Figure 2. Representative viscosity versus time plots of the films with thicknesses from 5 to 125 nm measured at temperatures between 130 and 160 °C. The solid line represents $\eta = 2 \times (10.5\ \text{kPa}) \times t$.

the films with thickness in the nanometer range. It should therefore be understood that the values of μ_{plateau} and η obtained from this analysis are effective values. Below, we shall elaborate how by measuring the effective viscosity of the films with different thicknesses, the dynamic heterogeneity in the films can be inferred.

RESULTS AND DISCUSSION

Figure 1a shows the sequence of power spectral density (PSD) obtained from a 20 nm film annealed at 130 °C. For times between $1980 \le t \le 8880$ s, the PSD shows negligible change, attributable to the film being in the rubbery plateau regime. It should be remarked that the initial change seen between $t = 0$ and 1980 s is caused by the glass-to-rubber transition,[16,27] not accounted for by the present model (eqs 1−3). In the rubbery plateau where the film is elastic, the plateau shear modulus, μ_{plateau}, can be determined from the lower cutoff wavevector, q_{lc}, of the PSD[27] by using $\mu_{\text{plateau}} \approx [((dG^2(h)/dh^2) + \gamma q_{\text{lc}}{}^2)h^3 q_{\text{lc}}{}^2]/3$,[27] where the symbols are as defined above. From the data shown, $q_{\text{lc}} \approx 17 \pm 2\ \mu\text{m}^{-1}$ so $\mu_{\text{plateau}} \approx 7 \pm 3.5$ kPa. To find the viscosity, η, we fit the data to eqs 1 and 3 as detailed in the Theoretical Analysis section. The best fitted values of η are plotted versus t in Figure 1b. We label the data in the rubbery region by open symbols and those in the terminal flow region by solid symbols. As seen, the data in the rubbery region exhibit a linear t-dependence, in accord with our model prediction, $\eta = 2\ \mu_{\text{plateau}} t$ (see the Theoretical Analysis section). By fitting the open symbols to this expression, we obtain $\mu_{\text{plateau}} = 6 \pm 1$ kPa, in reasonable agreement with the value calculated from the lower cutoff wavevector. In the terminal flow regime (where the solid symbols are), the viscosity grows with time initially but reaches a saturated value after about 90 000 s. A growth in the viscosity of as-cast entangled polymer films upon annealing has also been observed by Barbero et al.[14] They ascribed the reduced viscosity found initially to a reduction in the entanglement density in the films due to rapid drying in the spin-coating process that could render the polymer chains insufficient time to attain the equilibrium conformation. Reduced entanglement density in the film is also in keeping with the noticeably smaller plateau modulus found here than the published bulk value, $\mu_{\text{plateau,bulk}}$ of 2×10^5 Pa.[13]

Figure 2 shows the representative η versus t data taken from the films with $h = 5-125$ nm upon annealing at $T = 130-160$ °C. The open and solid symbols denote the measurements taken

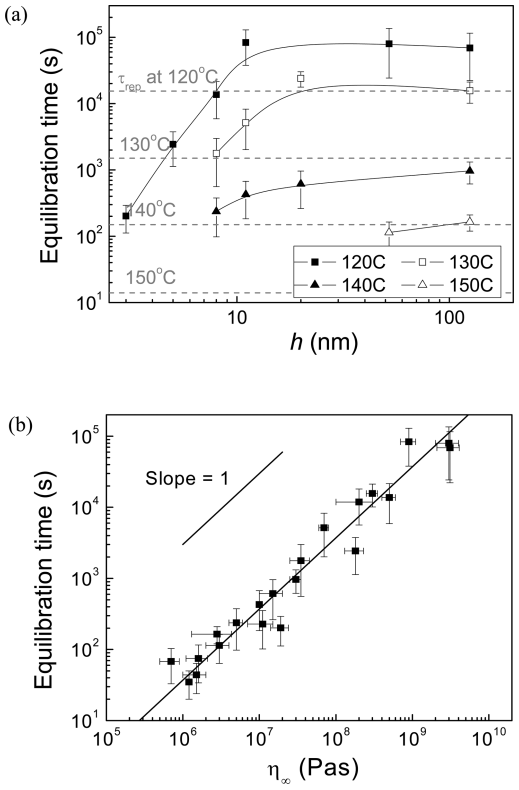

Figure 3. (a) Equilibration time versus film thickness measured at four temperatures between 120 and 150 °C. The gray dashed lines indicate the reptation times at these temperatures. (b) Equilibration time versus saturated viscosity of all the films measured in this experiment. The straight line is the best linear fit to the data.

during and after the rubbery regime, respectively. As seen, all the data in the rubbery regime exhibit a linear t-dependence as predicted above and found in Figure 1b. Remarkably, they essentially overlap, suggesting the films to have approximately the same μ_{plateau}. For polymers, the plateau modulus μ_{plateau} is related to the entanglement density, ρ_e, by $\mu_{\text{plateau}} = (4/5)\rho_e k_B T$.[28] The present finding means that despite the large variation in the thickness of the films and hence the concentration of the polymer solutions used to cast them, the films possess similar entanglement density initially.

We look further into this point by examining the equilibration time, τ_{eq}, for $\eta(t)$ to reach the saturated value. The dashed lines in Figure 1b demonstrate how τ_{eq} is determined from a plot of η versus t. Representative τ_{eq} obtained at measurement temperatures between 120 and 150 °C are plotted versus h in Figure 3a. The reptation times (τ_{rep})[12,28] of the bulk polymer at the respective temperatures, calculated by using $\tau_{\text{rep}} \approx \eta_{\text{bulk}}/\mu_{\text{plateau,bulk}}$,[12] are shown by the dashed lines (where η_{bulk} denotes the viscosity of the bulk polymer and $\mu_{\text{plateau,bulk}}$ is approximated by 2×10^5 Pa). As seen, when h is increased, τ_{eq} rises with increasing h and reaches τ_{rep} at $h \approx 8$ nm. As h exceeds ~20 nm, τ_{eq} begins to saturate. We find that the maximum value of τ_{eq} is typically $\sim 10\tau_{\text{rep}}$. In the reptation model,[28] τ_{rep} is the time for a polymer chain to escape the confinement arising from the nearby entanglement strains[28] that eventually causes the stress relaxation modulus of the entanglement chain network to decay to zero.[12] The fact that τ_{eq} can exceed τ_{rep} means that equilibration of the films must involve processes more than just escaping of the

dx.doi.org/10.1021/ma201675z |Macromolecules 2011, 44, 8294–8300

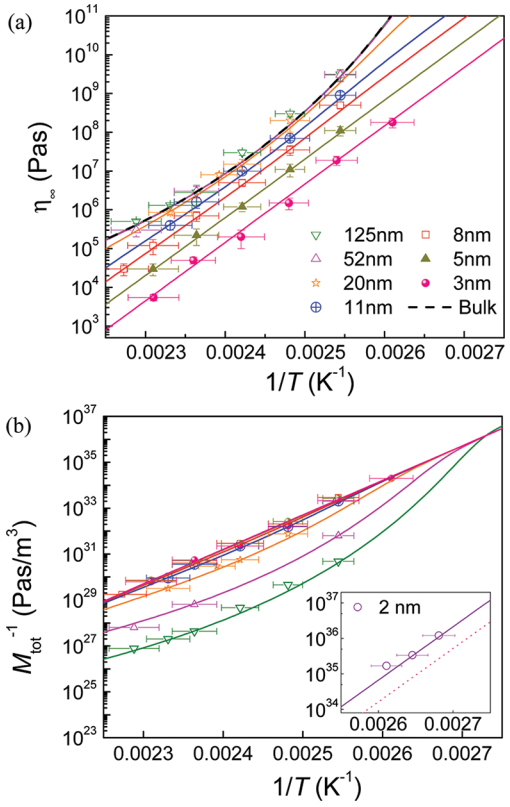

Figure 4. (a) Saturated viscosity of the films with thicknesses from 3 to 125 nm plotted versus reciprocal temperature (symbols). The dashed line represents the published data of the bulk polymer. The solid lines are the least-squares fits to the two-layer model as described in the text. (b) A plot of inverse mobility versus reciprocal temperature for the films shown in (a) (symbols). The solid lines are the least-squares fits to the two-layer model. Inset: corresponding plot of the data taken from a 2 nm film. The dashed line reproduces the collapsed behavior seen in the main panel. The solid line is $(2/3.3)^{-3}$ times the dotted line.

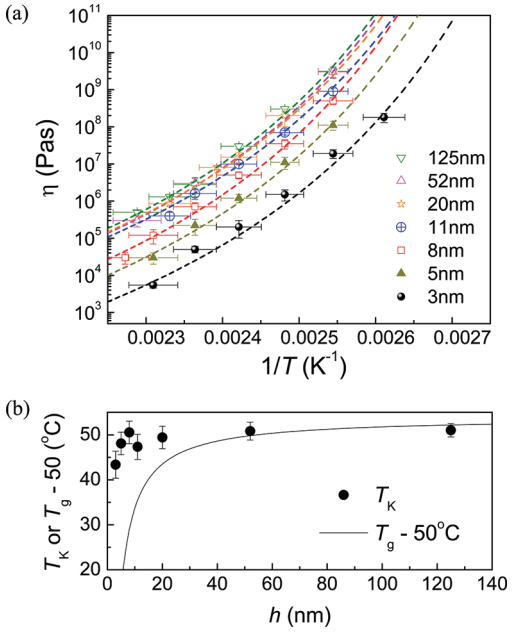

Figure 5. (a) Viscosity versus reciprocal temperature of PS films with different thicknesses as labeled in the legend (symbols). The dashed lines are the least-squares fits to the VFT relation,[11,38] $\eta = \eta_0 \exp[A/(T - T_K)]$, where both η_0 and T_K were covaried while A was fixed to 1620 K.[33] (b) The fitted values of T_K obtained from (a) plotted as a function of the film thickness (solid circles). The solid line represents the measured T_g of PS films (M_w = 393 kg/mol), as represented by least-squares fit to the model by Keddie et al.,[1] minus 50 °C.

polymer chains from the entanglement-induced confinement. Since the viscosity of entangled polymers increases with ρ_e, the rise in η with t beyond the rubbery region means that the equilibration also entails restructuring of the chain conformation to increase ρ_e. As noted above, τ_{eq} starts to break off from saturation when h falls below ~20 nm. We notice that 20 nm is also the thickness below which the thickness dependence of the T_g of the films begins to accelerate.[1,3,6,29] We examine if τ_{eq} and the long-time, saturated viscosity, η_∞, may be correlated by plotting τ_{eq} versus η_∞ in Figure 3b. We find that the data fit well to the relation, $\tau_{eq} = (10^{-4.4\pm0.45}\ \text{Pa}^{-1})\eta_\infty$ (solid line). Recall that τ_{eq} is determined by intersecting the $t \to 0$ (where $\eta = 2\mu_{plateau}t$) and $t \to \infty$ asymptotes of the $\eta(t)$ data (where $\eta = \eta_\infty$), so the result of Figure 3b implies that all the films have approximately the same median $\mu_{plateau}$ (≈12.6 kPa). It is noteworthy that reduced entanglement is also expected in ultrathin films where the film thickness is smaller than the gyration radius of the polymer, R_g (≈12 nm here), as demonstrated in the crazing experiment of Si et al.[30] The fact that the plateau moduli of all the films, including those with $h > R_g$ and $h < R_g$, are similar suggests that the reduced plateau modulus observed here is more likely to arise from the same conformational state (with reduced entanglement) being entrapped in the films at spin-coating than to confinement effects.

In spin-coating, the chain conformation that transpires at an intermediate concentration ϕ^* can get kinetically frozen-in as the film continues to dry and ϕ approaches 0.8 where the film vitrifies.[16] We estimate ϕ^* from the observed median $\mu_{plateau}$. It has been shown that the entanglement density, $\rho_e(\phi)$, of a polymer solution (made of an athermal solvent) with polymer concentration ϕ is given by $\rho_e(\phi) = \rho_e(1)\phi^{2.3}$,[12] where $\rho_e(1)$ is the entanglement density of the polymer melt at equilibrium. Upon kinetic freezing-in at ϕ^*, the chain conformation and the corresponding entanglement density $\rho_e(\phi^*)$ gets locked in. We assume that further drying of the film from this point causes the network to shrink uniformly without inducing conformational change. Upon complete drying, the film volume shrinks by a factor of $1/\phi^*$ whereupon ρ_e is increased by the same factor. Given this and the fact that $\mu_{plateau} \propto \rho_e$, we anticipate $\mu_{plateau}(\phi) = \mu_{plateau}(1)\phi^{*1.3}$ for the as-cast films. On substituting $\mu_{plateau}$ = 12.6 kPa and $\mu_{plateau}(1)$ = 100 kPa, we obtain ϕ^* = 0.2. We contemplate ϕ^* to be the concentration where kinetic slowing down in the dynamics of the polymer solution commences. Scaling argument[12] suggests that this should take place at a concentration of about $(M_e/M_w)^{0.76}$. By substituting $M_e \approx 17$ kg/mol[12] and M_w = 212 kg/mol, we obtain $\phi^* \approx 0.15$, which is in reasonably good agreement with the above estimate of ϕ^*, especially given that scaling arguments are known to give order-of-magnitude estimates only.

Figure 4a displays the long-time viscosity of the films, η_∞, plotted versus $1/T$. As one can see, the measurements of the $h \geq$ 20 nm films overlap with that of the bulk polymer, demonstrating that confinement effects are insignificant and the films have reached the equilibrium bulk entanglement density when η reaches the saturated value. In addition, η_∞ gets smaller and

diverges more slowly with $1/T$ as h decreases, both of which had been observed in unentangled PS films and are consistent with the T_g of the films decreasing with decreasing h.[11] With unentangled PS films,[11] we found that the Kauzmann temperature, T_K, obtained by fitting the $\eta(T)$ measurements to the Vogel−Fucher−Tammann (VFT) relation, exhibited good quantitative agreement with the T_g of the films. By applying the same analysis to the data of Figure 4a, we find that the T_K of our films also exhibits a reduction with decreasing h, but the thickness dependence is noticeably different from that of the T_g (see Figure 5). The difference is probably a reflection that the molecular motions determining the viscosity are not the same as those determining the glass transition. In particular, the former involves large-scale, chain reptation motions while the latter involves local, segmental motions. This is in keeping with a recent photobleaching experiment of free-standing PS films, where inconsistency between the molecular mobility and T_g was found.[31]

To understand the data of Figure 4a, we invoke the concept of (flow) mobility, M_{tot}, as we did before in analyzing the data of unentangled films.[11] By definition, mobility is the ratio of the total horizontal current in the film to the pressure gradient causing it.[11] As pointed out before,[11] M_{tot}, rather than η, is a fundamental parameter of our model. Specifically, ω_{liq} is actually $-M_{tot}[(dG^2(h)/dh^2)q^2 + \gamma q^4])$.[32] Only given our experimental conditions and the assumption that the films are homogeneous is $M_{tot} = h^3/(3\eta)$, whereupon $\omega_{liq} = -(h^3/(3\eta))[(dG^2(h)/dh^2)q^2 + \gamma q^4])$. In Figure 4b, we plot M_{tot}^{-1} ($\equiv 3\eta_\infty/h^3$) versus $1/T$ by using the measurements of η_∞ in Figure 4a. For the thick films with $h \geq 20$ nm, M_{tot} increases with increasing h, consistent with the relation between M_{tot} and h (i.e., $M_{tot} \equiv h^3/(3\eta_\infty)$), suggesting that the flow current should be bigger for thicker homogeneous films. Such prediction is intuitive because thicker films have more fluid and less drag so a bigger flow can be sustained for the same driving force. For the films with $h \leq 11$ nm, however, M_{tot} becomes independent of h, and collapses onto the Arrhenius dependence:

$$\frac{3\eta}{h^3} = ((4 \pm 1)\times 10^{-5}\ \mathrm{Pa\cdot s\cdot m^{-3}}) \exp\left(\frac{280 \pm 9\ \mathrm{kJ/mol}}{R(T + 273\ \mathrm{K})}\right) \quad (6)$$

where $R = 8.31$ J mol^{-1} K^{-1} is the gas constant. This counterintuitive observation can be naturally explained if a surface layer, with mobility, $M_{surface}$ given by eq 6 exists at the free surface and the rest of the film is bulklike and has the bulk viscosity, η_{bulk}. When h is big, the mobility of the bulklike layer ($\approx h^3/(3\eta_{bulk})$) is $\gg M_{surface}$ and dominates. But when h is small such that $h^3/(3\eta_{bulk})$ becomes less than $M_{surface}$, the surface layer dominates whereupon $M_{tot} \approx M_{surface}$ and independent of h. This shows that the surface mobile layer would impose a lower limit of $M_{surface}$ to M_{tot} (or an upper limit of $M_{surface}^{-1}$ to M_{tot}^{-1}), which is apparent in Figure 4b. We examine if the measurements of $\eta_\infty(T)$ and $M_{tot}(T)$ can be described by using the two-layer model employed before for unentangled PS films.[11] Specifically, we assume that the mobility of the films is equal to be the sum of the mobilities of the two layers, that is, $M_{tot}(T) = h^3/(3\eta_{bulk}(T)) + M_{surface}(T)$, and the effective viscosity of the film ($= \eta_\infty(T)$ here) is $h^3/(3M_{tot}(T))$. The former assumption has been justified before by solving the Navier−Stokes equation appropriate to the experiment and then applying the experimental parameters.[11] By using eq 6 for $M_{surface}(T)$ and the published values of $\eta_{bulk}(T)$,[33] we calculated $\eta_\infty(T)$ and $M_{tot}(T)$. As seen, the result, represented by the solid lines in Figure 4a,b, describes the measurements quite well.

The apparent success of the two-layer model in describing the data would imply that the surface mobile layer is inherent to the films at equilibrium and warrants further discussions. Our data show that the $M_{surface}(T)$ measurements of both the unentangled ($M_w = 2.4$ kg/mol) and entangled ($M_w = 212$ kg/mol) PS films can be described by Arrhenius dependence, with the dynamic activation energies being 185[11] and 280 kJ/mol, respectively. A smaller dynamic activation energy found in the surface layer with lower M_w may be caused by the monomeric friction coefficient there being smaller. A similar correlation has also been found in bulk polymers and attributed to the increase in the density of chain ends in the melt when M_w is decreased.[34] We also notice that the surface dynamic activation energies found here are notably smaller than those of the respective bulk polymers at the T_g, namely 270 and 425 kJ/mol, respectively.[35] Similar observation was also made by others studying the surface mobility of PS films.[31,36,37]

Besides the dynamic activation energy, we can also deduce the thickness of the surface mobile layer. The open circles in the inset of Figure 4b denote the $M_{tot}(T)^{-1}$ measurements of the films with thickness, $h = 2$ nm. The dotted line reproduces the collapsed $M_{tot}(T)^{-1}$ behavior shown in the main panel. Evidently, the $M_{tot}(T)^{-1}$ data of the 2 nm films lie above the dotted line. According to the two-layer model, collapse of $M_{tot}(T)$ is caused by its dominance by $M_{surface}(T)$, the mobility of the whole surface mobile layer. When the film thickness is decreased below the natural thickness of the surface mobile layer, $M_{tot}(T)$ should decrease with decreasing h. We find that the data of the 2 nm films can be described by the relation, $M_{tot}(T) = M_{surface}(T)(2/3.3)^3$ (solid line in the inset of Figure 4b), implying that the surface mobile layer of the films can be perceived as having an apparent thickness of ~3 nm. Since the prefactor of eq 6 is proportional to the amount of polymer material belonging to the surface mobile layer, the fact that this prefactor is a constant suggests that the apparent thickness of the surface mobile layer does not change with temperature over the temperatures studied.

Contrary to the VFT dynamics found of the bulk polymers, the Arrhenius dynamics observed here of the surface mobile layer correspond to simple, uncooperative motions, characteristic of systems with ample configurational entropy as found in simple liquids above the melting temperature.[38] The abundant configurational entropy apparent in the surface mobile layer is probably due to its proximity to the air interface whereby configurational changes can occur at lower energy costs. Varnik et al.[39] had used molecular dynamics (MD) simulations to study the dynamics of unentangled polymer films confined between smooth, repulsive walls. The monomer−wall interaction was made softer than that between the monomers, so the chain segments could have more freedom to move. Our current and previous[11] measurements show that the thickness of the surface mobile layer is no more than ~3 nm, corresponding to about 4 segmental lengths,[12,13] and independent of temperature. In the MD simulations,[39] a mobile, liquidlike interfacial layer, where the dynamics showed no caging effect, was also found within ~2 segmental lengths from the interfaces even at low temperatures where cooperative dynamics was clearly seen in the center of the melt film.[39] While the spatial extent of the perturbation to the local segmental relaxation rate was found to increase with decreasing temperature or progressive supercooling, the distance over which the size of the perturbation dropped by 90% was actually ~4 segmental lengths and showed little variation with temperature, as found here for the apparent thickness of the

surface mobile layer. The good agreement between the properties of the surface mobile layer found by MD simulations and by us endorses our association of the Arrhenius dynamics of the surface mobile layer to the enhanced freedom of segmental motions at the free surface.

Previous nanoparticle embedding[40] and reorientation relaxation after photobleaching[31] measurements found that the thickness of the surface region with enhanced mobility increased with increasing temperature. Local fluorescence label[10] and positron annihilation[8] experiments found that the thickness of the surface region with reduced T_g could exceed 20 nm.[8,10] These results appear to be inconsistent with the properties found here of the surface mobile layer and warrant discussions. We contemplate that different experiments probe different motions of the molecules that can have different surface sensitivity. This may also explain why the values probed by nanoparticle embedding[40] and reorientation relaxation after photobleaching[31] for the surface layer thickness disagree by a factor of ~2. In turn, these values are smaller than those probed by the local T_g measurements[8,10] by an order of magnitude.

By monitoring the diffusive motion of nanogold particles with X-ray photon correlation spectroscopy (XPCS), Koga et al.[41] found evidence of enhanced surface mobility in PS films at temperatures above the T_g, which we also found here and previously.[11] But unlike us,[11] Koga et al. did not observe any enhanced surface mobility in the films with $M_w \leq 30$ kg/mol (Figure 4 of ref 41). Moreover, the size of enhancement they found at 156 °C was less than 2-fold (Figure 4 of ref 41) while that found here is more than 100-fold (Figure 4b). We tentatively address these differences by considering the experimental parameters. In Koga et al.'s experiment,[41] the diameter of the nanoparticles used was 5.6 nm while the thickness of the surface mobile layer estimated here is ≈3 nm. Given these, part of the nanoparticles is embedded in the transition region between the surface layer and the bulklike inner region beneath. Embedment in the transition region can cause the diffusive motion of the particles to slow down and the measured surface viscosity to be substantially raised. As for the lack of surface-mobility enhancement Koga et al.[41] found in the films with $M_w \leq 30$ kg/mol, one possible reason is that the mobility enhancement they saw was due to reduced entanglement at the free surface, which is expected from packing constraints of polymer chains at the free surface (or, more generally, a reflective wall).[29,30] On the basis of the result of ref 14 and ours above, adjustment to the viscosity due to reduced entanglement is expected to be between 1 and 10, which agrees well with Koga et al.'s observation. Correspondingly, the much bigger mobility enhancement we observed must arise from a different origin. At this time, we think that it originates from the greater configurational entropy enabled by the free surface as discussed above, in keeping with predictions by MD simulations.[39]

It is worth noting that the surface layer thickness found here (~3 nm) is only 1/4 times the R_g (≈12 nm) of the entangled polymer used in this experiment. This would imply that the top 3 nm portion of the molecule belongs to the surface mobile layer and follows the Arrhenius dynamics while the rest of the molecule belongs to the bulklike inner layer and follows the VFT dynamics of the bulk. Because of the large disparity between the dynamics of the two layers, as surface capillary waves develop on the film surface the surface chains would become shear deformed—a situation akin to that of a polymer brush under the excitation of a surface capillary wave.[26] Following the approach of Fredrickson et al.,[26] we estimate that the lateral displacement, δx, of the polymer near the top of the films is $\sim \delta h/(qh_t)$, where $h_t \approx 3$ nm is the thickness of the surface layer, δh is the amplitude, and q is the wavevector of the surface capillary wave. By substituting the average experimentally observed rms roughness of the films for δh and assuming $1/q \sim 1$ μm (this is the order of magnitude of the longest-wavelength capillary wave typically observed in experiment), we obtain $\delta x \approx 126$ nm. In the above, we have neglected the lateral displacement in the bulklike inner layer because it should be comparative smaller ($<\delta x/10$ if diffusion prevails and so lateral displacement scales with the local viscosity η according to $\sim \eta^{-1/2}$). It follows that the surface chains are stretched by an amount $\approx \delta x$, for which the stretching energy per chain is $\sim k_B T \delta x^2/R_g^2$ or $103 k_B T$ in here. It is difficult to perceive how capillary modes entailing such a large stretching energy can be excited, as no external force was applied and all the capillary modes were thermally excited. One possibility is that the polymer chains at the free surface actually do not extend into the bulklike inner layer. It has been suggested that polymer chains near a reflective surface are oblate, with the dimension perpendicular to the substrate ($R_\perp$) being less than R_g and that parallel to the substrate ($R_\parallel$) the same as R_g.[42] Theory predicts that $R_\perp \approx 0.603 R_g$.[42] But in here, it needs to be $\sim 0.25 R_g$ in order for the surface chains to be independent of the bulklike inner layer and chain stretching unnecessary. At this time, we do not know if this level of agreement is adequate for the picture of oblate deformation of the surface chains to be acceptable. If it is not, a mechanism completely different from the two-layer model is necessary to explain our observations. This model, whatever it is, must be able to explain why η_∞ follows the $\sim 1/h^3$ scaling and the total mobility is a constant for $h < \sim 20$ nm. All these issues are important and will be addressed in a future study.

In conclusion, we have measured the evolution in the viscoelastic dynamics of as-cast PS films with $M_w = 212$ kg/mol and thickness $h = 2-125$ nm upon annealing above the T_g. Our measurements reveal that the initial chain conformation in the films was substantially far from equilibrium, with an entanglement density only ~1/10 times the bulk value. Upon annealing above the T_g, the chain conformation evolved to increase the density of entanglement. In the steady state, the viscosity of the films stabilized at a saturated value, η_∞ found to be the same as the bulk for the thick films with $h > \sim 20$ nm. For the thin films with $3 \leq h < 20$ nm, η_∞ decreased with decreasing h and their mobility, $M_{tot} = h^3/3\eta_\infty$, collapsed onto an Arrhenius temperature dependence. By using the two-layer model employed before for unentangled films, we were able to fully describe the η_∞ measurements. A straightforward interpretation of this result implies that the surface mobile layer exists in the films at equilibrium and determines the dynamics of unentangled and entangled films in a similar way. However, a more detailed analysis reveals that this picture would require the surface chains to be oblate with the dimension perpendicular to the film being no more than 1/4 times the unperturbed gyration radius of the polymers for otherwise it would lead to unphysically large stretching of the surface chains. Further studies are necessary to investigate the feasibility of the two-layer model more fully.

AUTHOR INFORMATION

Corresponding Author

*E-mail: okctsui@bu.edu.

Present Addresses
[§]Center for Soft Condensed Matter Physics & Interdisciplinary Research, Soochow University, Suzhou 215123, P. R. China.

■ ACKNOWLEDGMENT

We acknowledge illuminating discussions with Kari Dalnoki-Veress and Jörg Baschnagel. Assistance from Nancy R. Li and Dongdong Peng is also acknowledged. This work is supported by the NSF under projects DMR-0908651 and DMR-1004648.

■ REFERENCES

(1) Keddie, J. L.; Jones, R. A. L.; Cory, R. A. *Eur. Phys. Lett.* **1994**, *27*, 59–64.
(2) Alcoutlabi, M.; McKenna, G. B. *J. Phys.: Condens. Matter* **2005**, *17*, R461–R524.
(3) Forrest, J. A.; Dalnoki-Veress, K. *Adv. Colloid Interface Sci.* **2001**, *94*, 167–196.
(4) Baschnagel, J.; Varnik, F. *J. Phys.: Condens. Matter* **2005**, *17*, R851–R953.
(5) Roth, C. B.; Dutcher, J. R. *J. Electroanal. Chem.* **2005**, *584*, 13–22.
(6) Tsui, O. K. C.; Zhang, H. F. *Macromolecules* **2001**, *34*, 9139–9142.
(7) Clough, A.; Peng, D.; Yang, Z.; Tsui, O. K. C. *Macromolecules* **2011**, *44*, 1649–1653.
(8) Glynos, E.; Frieberg, B.; Oh, H.; Liu, M.; Gidley, D. W.; Green, P. F. *Phys. Rev. Lett.* **2011**, *106*, 128301.
(9) DeMaggio, G. B.; Frieze, W. E.; Gidley, D. W.; Zhu, M.; Hristov, H. A.; Yee, A. F. *Phys. Rev. Lett.* **1997**, *78*, 1524–1527.
(10) Ellison, C. J.; Torkelson, M. *Nature Mater.* **2003**, *2*, 695–670.
(11) Yang, Z.; Fujii, Y.; Lee, F. K.; Lam, C.-H.; Tsui, O. K. C. *Science* **2010**, *328*, 1676–1679.
(12) Rubinstein, M.; Colby, R. H. *Polymer Physics*; Oxford University Press: New York, 2003.
(13) Strobl, G. R. *The Physics of Polymers*; Springer-Verlag: Berlin, Germany, 1996.
(14) Barbero, D. R.; Steiner, U. *Phys. Rev. Lett.* **2009**, *102*, 248303.
(15) Raegen, A.; Chowdhury, M.; Calers, C.; Schmatulla, A.; Steiner, U.; Reiter, G. *Phys. Rev. Lett.* **2010**, *105*, 227801.
(16) Tsui, O. K. C.; Wang, Y. J.; Lee, F. K.; Lam, C.-H.; Yang, Z. *Macromolecules* **2008**, *41*, 1465–1468.
(17) Fujii, Y.; Yang, Z.; Leach, J.; Atarashi, H.; Tanaka, K.; Tsui, O. K. C. *Macromolecules* **2009**, *42*, 7418–7422.
(18) Napolitano, S.; Wubbenhorst, M. *Nature Commun.* **2011**, *2*, 260–266.
(19) Wang, Y. J.; Tsui, O. K. C. *Langmuir* **2006**, *22*, 1959–1963.
(20) Wang, Y. J.; Tsui, O. K. C. *J. Non-Cryst. Solids* **2006**, *352*, 4977–4982.
(21) Wang, Y. J.; Lam, C.-H.; Zhang, X.; Tsui, O. K. C. *Eur. Phys. J. Spec. Top.* **2007**, *141*, 181–187.
(22) Yang, Z.; Lam, C.-H.; DiMasi, E.; Bouet, N.; Jordan-Sweet, J.; Tsui, O. K. C. *Appl. Phys. Lett.* **2009**, *94*, 251906.
(23) Peng, D.; Yang, Z.; Tsui, O. K. C. *Macromolecules* **2011**.
(24) Zhao, H.; Wang, Y. J.; Tsui, O. K. C. *Langmuir* **2005**, *21*, 5817–5824.
(25) Safran, S. A.; Klein, J. *J. Phys. II* **1993**, *3*, 749–757.
(26) Fredrickson, G. H.; Ajdari, A.; Leibler, L.; Carton, J.-P. *Macromolecules* **1992**, *25*, 2882–2889.
(27) Yang, Z. H.; Wang, Y.; Todorova, L.; Tsui, O. K. C. *Macromolecules* **2008**, *41*, 8785–8788.
(28) Doi, M.; Edwards, S. F. *The Theory of Polymer Dynamics*; Clarendon Press: Oxford, 1986.
(29) Tsui, O. K. C.; Russell, T. P.; Hawker, C. J. *Macromolecules* **2001**, *34*, 5535–5539.
(30) Si, L.; Massa, M. V.; Dalnoki-Veress, K.; Brown, H. R.; Jones, R. A. L. *Phys. Rev. Lett.* **2005**, *94*, 127801.
(31) Paeng, K.; Swallen, S. F.; Ediger, M. D. *J. Am. Chem. Soc.* **2011**, *133*, 8444–8447.
(32) Vrij, A.; Overbeek, J. T. G. *J. Am. Chem. Soc.* **1968**, *90*, 3074–3078.
(33) Majeste, J.-C.; Montfort, J.-P.; Allal, A.; Marin, G. *Rheol. Acta* **1998**, *37*, 486–499.
(34) O'Connor, K. M.; Scholsky, K. M. *Polymer* **1989**, *30*, 461–466.
(35) Santangelo, P. G.; Roland, C. M. *Macromolecules* **1998**, *31*, 4581–4585.
(36) Tanaka, K.; Takahara, A.; Kajiyama, T. *Macromolecules* **2000**, *33*, 7588–7593.
(37) Fakhraai, Z.; Forrest, J. A. *Science* **2008**, *319*, 600–604.
(38) Angell, C. A.; Ngai, K. L.; McKenna, G. B.; McMillan, P. F.; Martin, S. W. *J. Appl. Phys.* **2000**, *88*, 3113–3157.
(39) Varnik, F.; Baschnagel, J.; Binder, K. *Phys. Rev. E* **2002**, *65*, 021507.
(40) Ilton, M.; Qi, D.; Forrest, J. A. *Macromolecules* **2009**, *42*, 6851–6854.
(41) Koga, T.; Li, C.; Endoh, M. K.; Koo, J.; Rafailovich, M.; Narayanan, S.; Lee, D. R.; Lurio, L. B.; Sinha, S. K. *Phys. Rev. Lett.* **2010**, *104*, 066101.
(42) Brown, H.; Russell, T. P. *Macromolecules* **1996**, *29*, 798–800.